Title

Evaluating controls on planktonic foraminiferal geochemistry in the Eastern Tropical North Pacific

Authors

Gibson, Kelly Ann
Thunell, Robert C
Machain-Castillo, Maria Luisa
et al.

Publication Date

2016-10-01

DOI

10.1016/j.epsl.2016.07.039

Peer reviewed

Earth and Planetary Science Letters 452 (2016) 90–103

Contents lists available at ScienceDirect

Earth and Planetary Science Letters

www.elsevier.com/locate/epsl

Evaluating controls on planktonic foraminiferal geochemistry in the Eastern Tropical North Pacific

Kelly Ann Gibson [a,*], Robert C. Thunell [a], Maria Luisa Machain-Castillo [b], Jennifer Fehrenbacher [c], Howard J. Spero [c], Kate Wejnert [d], Xinantecatl Nava-Fernández [b], Eric J. Tappa [a]

[a] School of the Earth, Ocean, and Environment, University of South Carolina, Columbia, SC, 29205, USA
[b] Instituto de Ciencias del Mar y Limnología de México, Universidad Nacional Autónoma de México, Unidad Académia Procesos Oceánicos y Costeros, Circuito Exeriro s/n, Ciudad Universitaria, 04510, México DF, Mexico
[c] Department of Earth and Planetary Sciences, University of California Davis, Davis, CA 95616, USA
[d] Fernbank Science Center, Atlanta, GA 30307, USA

ARTICLE INFO

Article history:
Received 31 January 2016
Received in revised form 20 July 2016
Accepted 21 July 2016
Available online xxxx
Editor: D. Vance

Keywords:
foraminiferal geochemistry
Mg/Ca
Eastern Tropical North Pacific
water column hydrography
secondary calcite
pH/[CO_3^{2-}]

ABSTRACT

To explore relationships between water column hydrography and foraminiferal geochemistry in the Eastern Tropical North Pacific, we present $\delta^{18}O$ and Mg/Ca records from three species of planktonic foraminifera, *Globigerinoides ruber*, *Globigerina bulloides*, and *Globorotalia menardii*, collected from a sediment trap mooring maintained in the Gulf of Tehuantepec from 2006–2012. Differences in $\delta^{18}O$ between mixed-layer species *G. ruber* and *G. bulloides* and thermocline-dweller *G. menardii* track seasonal changes in upwelling. The records suggest an increase in upwelling during the peak positive phase of El Niño, and an overall reduction in stratification over the six-year period. For all three species, Mg/Ca ratios are higher than what has been reported in previous studies, and show poor correlations to calcification temperature. We suggest that low pH (7.6–8.0) and [CO_3^{2-}] values (~70–120 μmol/kg) in the mixed layer contribute to an overall trend of higher Mg/Ca ratios in this region. Laser Ablation Inductively Coupled Mass Spectrometry analyses of *G. bulloides* with high Mg/Ca ratios (>9 mmol/mol) reveal the presence of a secondary coating of inorganic calcite that has Mg/Ca and Mn/Ca ratios up to an order of magnitude higher than these elemental ratios in the primary calcite, along with elevated Sr/Ca and Ba/Ca ratios. Some of the samples with abnormally high Mg/Ca are found during periods of high primary productivity, suggesting the alteration may be related to changes in carbonate saturation resulting from remineralization of organic matter in oxygen-poor waters in the water column. Although similar shell layering has been observed on fossil foraminifera, this is the first time such alteration has been studied in shells collected from the water column. Our results suggest a role for seawater carbonate chemistry in influencing foraminiferal calcite trace element:calcium ratios prior to deposition on the seafloor, particularly in high-productivity, low-oxygen environments.

1. Introduction

Production in the Eastern Tropical Pacific (ETP) accounts for 10% of total global primary productivity (Pennington et al., 2006). As such, the region plays an important role in the global carbon cycle. In the Eastern Pacific Warm Pool (EPWP), changes in sea level pressure (SLP) gradients between the Atlantic and Pacific Ocean basins lead to wind-driven upwelling of nutrient-rich subsurface waters that support locally high primary productivity (Pennington et al., 2006). The impacts of future warming on SLP gradients and wind-driven upwelling are uncertain, with conflicting reports from different coastal systems (Garcia-Reyes et al., 2015). Continued warming will almost certainly influence productivity and ocean-atmosphere CO_2 fluxes in these regions. Reconstructions of water column hydrography can be used to assess SLP gradient-driven changes in upwelling in the past. These changes are key to understanding how warming trends will impact productivity and changes in the carbon cycle in this region in the future.

Foraminiferal Mg/Ca ratios are a widely used tool for reconstructing changes in water column temperature. Samples used in

* Corresponding author at: University of South Carolina, School of the Earth, Ocean and Environment, 701 Sumter St EWS 617, Columbia, SC, 29208, USA.
E-mail address: kgibson@geol.sc.edu (K.A. Gibson).

http://dx.doi.org/10.1016/j.epsl.2016.07.039
0012-821X/

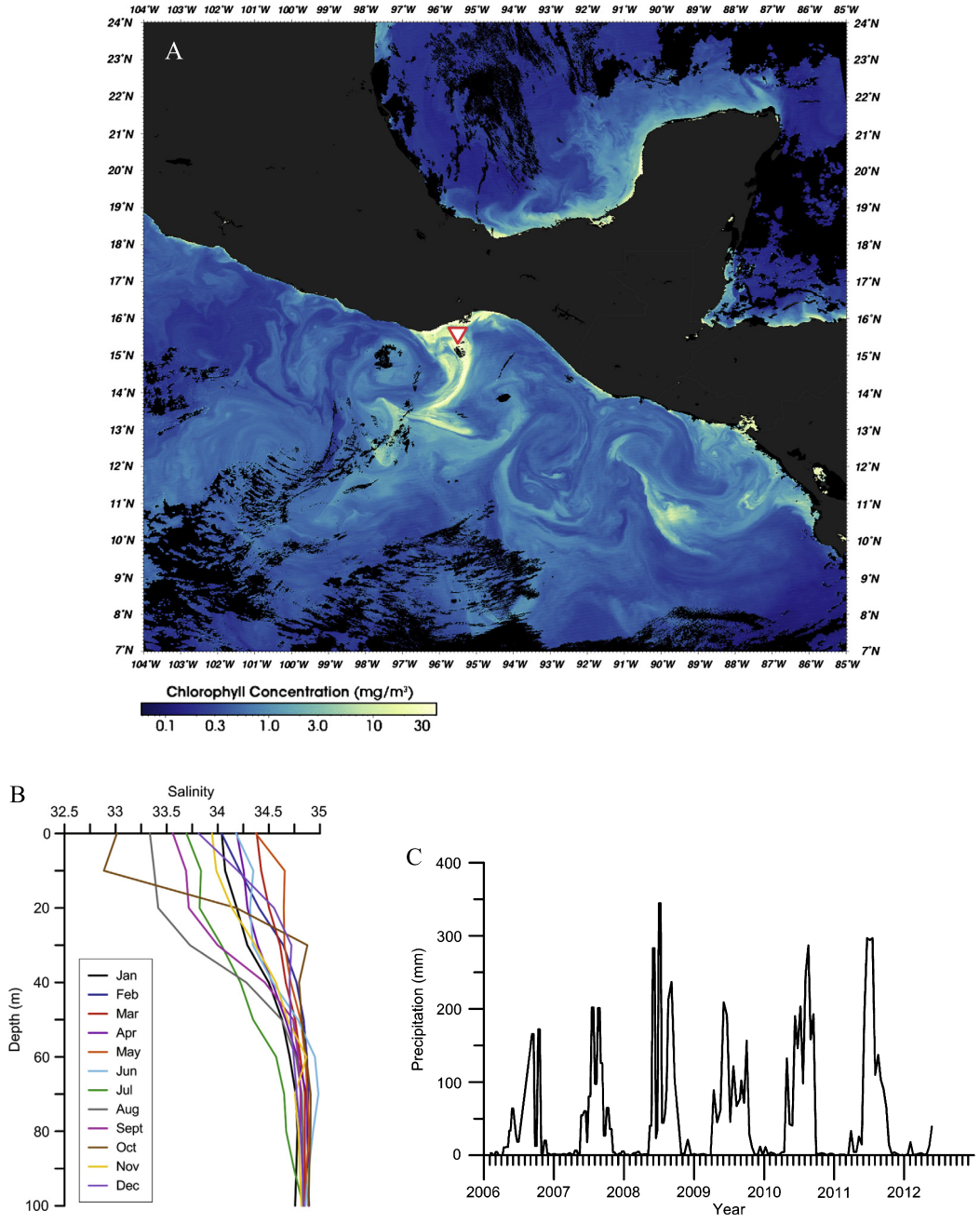

Fig. 1. Regional setting for the GoT sediment trap mooring. (A) January 2005 chlorophyll concentrations (http://oceancolor.gsfc.nasa.gov/cms/) associated with a "Tehuanos" wind event, with the location of the sediment trap mooring (white triangle). (B) Variation in salinity (WOA 13) throughout the year over the upper 100 m of the water column. (C) Biweekly precipitation totals for the study period from the TRMM satellite (Huffman et al., 2007).

the development and calibration of this proxy have come from laboratory culture, sediment traps, plankton tows and core-tops, and nearly all regions of the world's oceans. Consistent throughout all of these calibration studies is an exponential Mg/Ca ratio:temperature sensitivity of 8–10% change in ratio per °C (Anand et al., 2003; Bolton et al., 2011; Dekens et al., 2002; Lea et al., 1999; Martínez-Botí et al., 2011; Mashiotta et al., 1999; McConnell and Thunell, 2005; Regenberg et al., 2009). The influences of secondary factors such as salinity and carbonate chemistry are still being evaluated, and in many cases appear to be species – and/or region-specific (Arbuszewski et al., 2010; Dekens et al., 2002; Evans et al., 2016; Hertzberg and Schmidt, 2013; Hönisch et al., 2013; Kısakürek et al., 2008; Russell et al., 2004).

In this study we investigate the relationship between water column hydrography and the $\delta^{18}O$ and Mg/Ca signatures of three species of planktonic foraminifera, *Globigerinoides ruber, Globigerina bulloides*, and *Globorotalia menardii*, collected between 2006 and 2012 from a sediment trap moored in the Gulf of Tehuantepec (GoT), located in the EPWP (Fig. 1). The goal is to establish the utility of using these species to reconstruct water column hydrography and changes in upwelling in this region. *Globigerinoides ruber* records mixed-layer temperatures (Fairbanks et al., 1982) and is typically found in relatively low numbers throughout the year in the GoT, only dominating the assemblage during El Niño conditions (Machain Castillo, pers. comm.). *Globigerina bulloides* is the most abundant species of foraminifera in GoT surface sediments (Machain-Castillo et al., 2008), and is present throughout the year in sediment trap samples. Therefore, this species was selected to provide the most complete temporal coverage for this study, despite the fact *G. bulloides* often displays seasonal

variability in abundance or depth habitat, migrating between the mixed layer and upper thermocline (McConnell and Thunell, 2005; Wejnert et al., 2010). *Globorotalia menardii* typically resides between the mixed-layer and thermocline (Niebler et al., 1999). When shell geochemistry is compared among these species, insight may be gained into changes in the surface to thermocline temperature gradient during periods of mixing and stratification.

2. Regional setting

In boreal summer, when the Intertropical Convergence Zone (ITCZ) is in its northernmost position, the GoT is characterized by warm (sea surface temperatures of 29–32 °C) and wet conditions. More than 93% of annual precipitation falls between May and October, resulting in a decrease in surface salinity of up to 1.5 units. The Costa Rica Coastal Current (CRCC), which gets its low salinity waters from the Equatorial Counter Current, flows north along the coast and influences the GoT, contributing to reduced summer salinities. In boreal winter, the ITCZ shifts southward and northeasterly trade winds prevent the CRCC from reaching the GoT. Instead, the California Current moves southward along the coast, to the western end of the GoT (Molina-Cruz and Martinez-López, 1994) and regional conditions are cool and dry.

The most variable feature of winter climate in the GoT is "Tehuanos" wind events. These short-lived (several days) but intense (~15–20 $m\,s^{-1}$) events occur with a roughly ten-day periodicity, and lead to turbulent mixing and upwelling of subsurface waters, with sea surface temperatures (SST) under the wind jet as much as 8 °C cooler than surrounding waters (Stumpf, 1975). The dominant control on Tehuanos strength and occurrence is the wintertime SLP difference between the Gulf of Mexico and the Eastern Tropical North Pacific (ETNP). Tehuanos cause shear turbulent mixing-driven increases in productivity and complex patterns of cyclonic and anticyclonic circulation within the GoT (Fig. 1a) (Liang et al., 2009; Müller-Karger and Fuentes-Yaco, 2000).

Rates of primary production in the GoT are on the order of 350 $g\,C\,m^{-2}\,yr^{-1}$ (Antoine et al., 1996), higher than might otherwise be expected for the oligotrophic EPWP, whose warm surface waters are influenced by neither the Northern Hemisphere nor Southern Hemisphere subtropical gyre circulations (Pennington et al., 2006). This physical isolation from the major gyre circulation results in poor water column ventilation that, combined with high rates of primary production and remineralization of sinking organic matter, results in a well-defined oxygen-minimum zone (OMZ) between 200–800 m water depth. Reduced oxygen concentrations occur at depths of 25–40 m in the GoT, and concentrations <0.5 ml/L are observed above 75 m water depth (Perez-Cruz and Machain-Castillo, 1990).

3. Materials and methods

3.1. Sediment trap sample $\delta^{18}O$ and Mg/Ca analyses

Between February 2006 and May 2012, a sediment trap mooring was maintained by the Universidad Nacional Autónoma de México (UNAM) and the University of South Carolina (USC) in the GoT (15.6°N, 95.3°W). Two sediment traps, at 450 and 550 m water depth, collected samples at weekly to biweekly intervals. Sediment trap turnaround cruises were limited by ship availability, resulting in missed sampling during the summer and data gaps within the time series (July 2007, 2008, and 2010, and August 2006–2009). Sediment trap cups were prepared with a 3% formalin solution and buffered with sodium borate to a pH of 8.0–8.5 to prevent oxidation of organic matter and associated pH changes. The collection periods of the top and bottom traps were staggered, and samples from overlapping collection periods are treated as replicates.

For samples with ample material, *G. bulloides* (>150 µm, average of 85 individuals picked per sample), *G. ruber* (250–355 µm, average of 35 individuals picked per sample), and *G. menardii* (300–400 µm, average of 21 individuals picked per sample) were picked to yield ~80–100 µg of material for $\delta^{18}O$ analysis and ~80–100 µg of material for Mg/Ca analysis. For *G. ruber*, both *G. ruber sensu stricto* (*ss*) and *G. ruber sensu lato* (*sl*) were combined for analysis, due to low abundance in most samples throughout the study period. Variations in both $\delta^{18}O$ and Mg/Ca between the two morphotypes have been reported (Steinke et al., 2005; Wang, 2000), although a recent sediment trap study suggests that $\delta^{18}O$ values between the two morphotypes are statistically indistinguishable (Thirumalai et al., 2014). Nonetheless, we acknowledge combining the morphotypes may contribute to variability in the *G. ruber* analyses.

Prior to $\delta^{18}O$ analyses, samples were briefly (30 s) sonicated in methanol and dried at 40 °C. Samples were run on a GV IsoPrime Isotope Ratio Mass Spectrometer equipped with a Multicarb sample preparation system, corrected to NBS-19 or an in-house Carrera Marble standard, and reported relative to Vienna Pee Dee Belemnite (V-PDB). Long-term instrument precision is ±0.06‰ for $\delta^{18}O$ ($\pm 1\sigma$) and sample reproducibility, based on duplicate analysis of sample splits is ±0.25‰ for *G. bulloides* ($n = 87$), ±0.25‰ for *G. ruber* ($n = 20$), and, ±0.21‰ for *G. menardii* ($n = 31$).

Sample preparation for Mg/Ca analysis followed the cleaning method of Barker et al. (2003), without inclusion of the reductive step. Clean samples were dissolved in an appropriate volume of 5% HNO_3^- to achieve [Ca] ~80 ppm, and run on a Jobin Yvon Ultima Inductively Coupled Plasma-Atomic Emission Spectrophotometer. The majority of samples were analyzed for Ca and Mg, with Mn and Fe added to later runs to monitor for contamination. Two samples had Mn/Ca ratios >0.100 µmol/mol, above the accepted threshold for contamination, and were not included in the final time series. Samples were corrected to an internal standard (SCP-19) run between every sample, and the interlaboratory standard ECRM 752-1 was analyzed for run validation. Instrument precision is ±0.04 mmol/mol for Mg/Ca, ±0.01 for Fe/Ca and ±0.02 mmol/mol for Mn/Ca. Sample reproducibility based on duplicate analysis of sample splits is ±0.4 mmol/mol for *G. bulloides* ($n = 67$) ±0.6 mmol/mol for *G. ruber* ($n = 11$), and ±0.7 mmol/mol for *G. menardii* ($n = 19$).

3.2. Scanning electron microscopy and LA-ICPMS analysis

Several specimens of *G. bulloides* from samples with high Mg/Ca ratios (>9 mmol/mol) appeared more thickly calcified when viewed under a dissecting microscope. A selection of individuals from samples with high (>9 mmol/mol), intermediate (6–8 mmol/mol), and low (<6 mmol/mol) Mg/Ca ratios were examined using scanning electron microscopy (SEM) to investigate variability in calcification and/or morphotype. Samples were mounted on carbon tape on SEM stubs, coated in gold, and analyzed with a Tescan Vega-3 SEM at the USC Electron Microscopy Center. Several individuals from each sample were analyzed for intrashell element variability at UC Davis using Laser Ablation Inductively Coupled Mass Spectrometry (LA-ICPMS).

Prior to LA-ICPMS analysis, individual *G. bulloides* were cleaned in a 1:1 solution of 30% H_2O_2 and 0.1N NaOH for 10 min at ~65 °C to remove remnant organics (Mashiotta et al., 1999), rinsed repeatedly in Milli-Q H_2O and placed on double-sided carbon tape on glass slides with the aperture side up. Trace element profiles were obtained using a Teledyne Photon Machines Analyte G2 193 nm excimer laser with a HelEx dual-volume laser ablation cell coupled to an Agilent 7700× quadrupole-ICP-MS. Isotopes (^{24}Mg,

Table 1
Equations used to determine calcification depth for *G. bulloides*, *G. ruber*, and *G. menardii*.

Equation	Species	T (°C) =	Calibration temp (°C)	$\delta^{18}O_{sw}$ correction (VSMOW to VPDB)	Reference
2	*N/A*	$16.9-4.38(\delta^{18}O_c-\delta^{18}O_{sw}) + 0.10(\delta^{18}O_c-\delta^{18}O_{sw})^2$		−0.20‰	O'Neil et al. (1969)
3	*G. ruber* (*O. universa* HL)	$14.9-4.80(\delta^{18}O_c-\delta^{18}O_{sw})$	15–25	−0.27‰	Bemis et al. (1998)
4	*G. ruber*	$14.2-4.44(\delta^{18}O_c-\delta^{18}O_{sw})$	16–31	−0.27‰	Mulitza et al. (2003)
5	*G. bulloides*	$13.2-4.89(\delta^{18}O_c-\delta^{18}O_{sw})$	15–25	−0.27‰	Bemis et al. (1998)
6	*G. bulloides*	$14.62-4.70(\delta^{18}O_c-\delta^{18}O_{sw})$	2–25	−0.27‰	Mulitza et al. (2003)
7	*G. menardii*	$14.6-5.03(\delta^{18}O_c-\delta^{18}O_{sw})$	22–29	−0.20‰	Bouvier-Soumagnac and Duplessy (1985)
8	*G. menardii*	$14.9-5.13(\delta^{18}O_c-\delta^{18}O_{sw})$		−0.27‰	Spero et al. (2003)

^{25}Mg, ^{27}Al, ^{43}Ca, ^{44}Ca, ^{55}Mn, ^{88}Sr, and ^{138}Ba) were measured using a rapid peak hopping procedure, and element/Ca ratios for the foraminifera were calculated offline in MS Excel, following established data reduction protocols (Longerich et al., 1996) that includes screening for outliers, drift correcting by bracketing samples with NIST SRM 610 analyses, and subtracting average background counts (calculated with the laser off) from each data point. In addition to sample analysis, a fossil *Orbulina universa* was analyzed to assess depth profile reproducibility (Fehrenbacher et al., 2015). Reproducibility of the mean Mg/Ca ratio of repeat measurements of *G. bulloides* is ~0.3 mmol/mol and %RSD of repeat measurements is ~5%. Long-term reproducibility of the mean Mg/Ca ratio of repeat analyses of the UCD *O. universa* (UCD-Ou4) laboratory standard is ~8%. Results from SEM and LA-ICPMS analysis are presented for representative samples with "low," "intermediate," and "high" Mg/Ca. These samples were chosen to demonstrate potential end members and range of solution Mg/Ca values, shell calcification, and geochemical variability.

3.3. Hydrographic datasets

We utilized several datasets representing physical and chemical water column properties. For SST we used Level 3 data from the AQUA-MODIS satellite (OBPG, 2002) at a 1 km^2 – resolution, centered on 15°38.8′N, 95°16.9′W (X. Nava, pers. comm.). Data are averaged biweekly to match the predominant trap collection interval. For sea surface salinity (SSS) between 2011–2012, we used the Aquarius Satellite (PO.DAAC; ftp://podaac.jpl.nasa.gov/allData/aquarius/) Level 3 data, at 1° resolution, centered on 15°N and 95°W, averaged biweekly. For data prior to 2011, average monthly salinity was calculated from World Ocean Atlas (WOA) 05 at 1° resolution, centered on 15.5°N, 95.5°W (Antonov et al., 2006), from WOA 13 (Zweng et al., 2013) at 0.25° resolution centered on 15.625°N, 95.375°W, and Aquarius SSS. For depth profiles, we used temperature and salinity data at 10 m intervals between 0–100 m in the water column from the WOA 13 database. Finally, we calculated one year's worth of seasonal (DJF, MAM, JJA, SON) regional [CO_3^{2-}] and pH values for the upper 100 m of the water column with carbon (TCO_2 and total alkalinity) and nutrient (Goyet et al., 2000) and hydrographic (WOA 13) data at 15.5°N 95.5°W using the CO2SYS program (Pelletier et al., 2005), with constants from Mehrbach et al. (1973) modified by Dickson and Millero (1987) and pH on the Seawater scale (mol kg^{-1} SW).

3.4. Calculating habitat depth and calcification temperatures

To determine calcification depth for each species, we first calculated $\delta^{18}O_{sw}$ for water depths between 0–100 m at 10 m intervals, using WOA 13 salinity. Seawater $\delta^{18}O$ was calculated using a SSS:$\delta^{18}O_{sw}$ relationship from the Panama Bight (Benway and Mix, 2004):

$$\delta^{18}O_{sw} = 0.253 * S - 8.52 \quad (1)$$

The resultant $\delta^{18}O_{sw}$ values agree within an average of ±0.04‰ with $\delta^{18}O_{sw}$ from the gridded global seawater $\delta^{18}O$ database (LeGrande and Schmidt, 2006). The $\delta^{18}O_{sw}$:salinity relationship should be valid for the mixed layer; however, there is considerable variability in salinity in the upper 50 m of the water column in the GoT (Fig. 1b), which may introduce some error to our calculations. We then determined predicted equilibrium $\delta^{18}O_{calcite}$ at each depth using several equations that relate calcification temperature to $\delta^{18}O_{calcite}$ (Table 1). We subtract 0.20–0.27‰ from $\delta^{18}O_{sw}$ (SMOW) in the temperature:$\delta^{18}O_{calcite}$ relationship to account for differences between the V-SMOW and V-PDB scales for these paleotemperature equations (Bemis et al., 1998).

4. Results

4.1. Foraminiferal $\delta^{18}O$ and Mg/Ca

The seasonal range in $\delta^{18}O$ is 3.37‰ (−3.52‰ to −0.15) for *G. bulloides*, 2.22‰ for *G. ruber* (−3.72‰ to −1.50‰), and 2.22‰ for *G. menardii* (−2.59‰ to −0.37‰). The *G. bulloides* and *G. ruber* records generally follow the seasonal pattern of SST, particularly at the lower range of $\delta^{18}O$ values (Fig. 2a). The lowest $\delta^{18}O$ values for *G. ruber* and *G. bulloides* occur between August–October of each year, coincident with or just following peak SSTs and precipitation. Highest values are observed in November–December and/or February–March of each year, corresponding to the beginning and end of the upwelling season. The $\delta^{18}O$ values for *G. menardii* are on average, 1.28‰ higher than the $\delta^{18}O$ of the two mixed-layer dwellers. Seasonal variability is also observed in the *G. menardii* record, with lower values during the summer/fall, and higher values during the winter/spring.

The Mg/Ca ratios range from 4.32 to 11.08 mmol/mol (average 6.29 mmol/mol) for *G. bulloides*, 4.80 to 10.43 mmol/mol for *G. ruber* (average 6.73 mmol/mol), and 2.62–5.01 mmol/mol for *G. menardii* (average 3.42 mmol/mol) (Fig. 2b). As with the $\delta^{18}O$ records, the Mg/Ca records for *G. bulloides* and *G. ruber* track each other well and display clear seasonal variations, although data from the summer months is scarce. The patchy nature of the *G. menardii* Mg/Ca record makes it difficult to comment on seasonal variability, but in general, the amplitude of variation is much less for the mixed-layer dwellers.

4.2. SEM images

The photomicrographs of the high (>9 mmol/mol) and intermediate (<6 mmol/mol) Mg/Ca specimens reveal the presence of a calcite precipitate on the test surface (Fig. 4b, c). Based on the crystal structure, the calcite overgrowth appears to be inorganic (Bolton et al., 2011; Hathorne et al., 2009) and is thicker than the chamber calcite. This secondary layer is not present in the *G. bulloides* specimen with low Mg/Ca (Fig. 4a). Additional samples with Mg/Ca values >6 mmol/mol (not shown) were examined under SEM and displayed secondary calcification of varying extent and

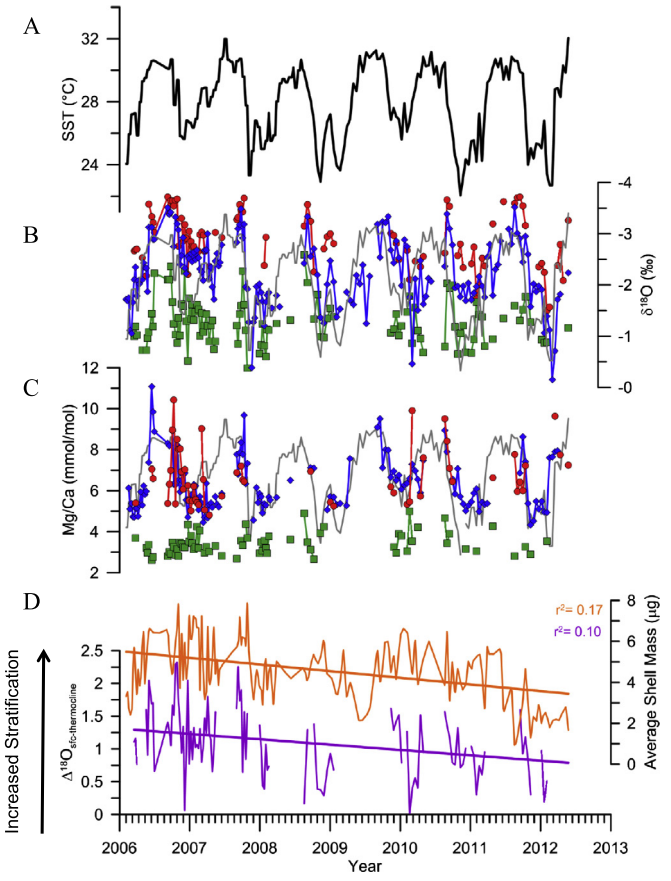

Fig. 2. (A) SST (AQUA-MODIS), (B) δ^{18}O for *G. ruber* (red), *G. bulloides* (blue), and *G. menardii* (green) with SST in gray, and (C) Mg/Ca for *G. ruber* (red), *G. bulloides* (bulloides), and *G. menardii* (green) with SST in gray for the full time series. (D) Shell weight for *G. bulloides* (purple) and surface-thermocline δ^{18}O gradient between *G. ruber*/*G. bulloides* and *G. menardii* (orange). Higher numbers indicate increased stratification. Trend lines are linear regressions. (For interpretation of the references to color in this figure legend, the reader is referred to the web version of this article.)

thickness, suggesting that secondary alteration of foraminiferal calcite may be pervasive in the GoT.

4.3. LA-ICPMS

The *G. bulloides* shells analyzed with LA-ICPMS display large interchamber element/Ca variability (Fig. 5). Within each shell, Mg/Ca ratios generally decrease in subsequent chambers, consistent with previous studies (Anand and Elderfield, 2005; Bolton et al., 2011). There is an average 31% reduction in Mg/Ca observed between the penultimate and final chamber, nearly identical to what is seen in *G. bulloides* tests from the southwest Pacific Ocean (Marr et al., 2011). Within each sample, substantial variability (average %RSD = 52%) is observed among single-specimen Mg/Ca ratios (taken as the average of chambers f through f-2). When the individuals from a sample are averaged together ($n = 3$), however, the ratios agree very well (average %RSD = 8%) with the ratios from samples analyzed via solution based ICP-AES, which each consisted of 40–50 dissolved *G. bulloides* specimens (average %RSD = 7%).

In unaltered samples, Mg/Ca ratios increase toward the inside of the chamber, while Sr/Ca, Ba/Ca, and Mn/Ca ratios are low and relatively unvarying (Figs. 5a–5d). For altered shells, the inorganic precipitate is characterized by Mg/Ca, Mn/Ca, and Ba/Ca values that are highly variable and up to an order of magnitude higher than ratios in the primary ontogenetic calcite (Figs. 5e–5l). Altered shells also display intrashell variability in the Sr/Ca ratios, which is atypical for foraminiferal calcite. While the single spot average ratios for Mn/Ca in altered foraminifera (0.02–0.05 µmol/mol) are higher than those without (0.01–0.03 µmol/mol), they are well below the Mn/Ca threshold for contamination (100 µmol/mol) (Supplementary Content). The Ba/Ca ratios, on the other hand, are clearly elevated in the foraminifera with the secondary precipitate relative to those without, and much higher than predicted for *G. bulloides* calcified in open ocean seawater conditions (Hönisch et al., 2011).

5. Discussion

5.1. Foraminiferal habitat depths and calcification temperatures in the GoT

The ranges in depth habitats based on calculated $\delta^{18}O_{sw}$ and predicted equilibrium $\delta^{18}O_{calcite}$ for each species are illustrated in Fig. 3. Based on the combined range in values and differences in results from equations listed in Table 1, for *G. bulloides*, we find an average calcification depth of ~30 m and a range of 0–50 m, for *G. ruber*, an average calcification depth of ~15 m with a range of 0–35 m, and an average calcification depth of ~40 m for *G. menardii* with a range of 15–75 m. These depths put *G. ruber* in the mixed layer, *G. bulloides* in the mixed layer/upper thermocline, and *G. menardii* in the thermocline, in agreement with accepted depth preferences for each species (Fairbanks et al., 1982; Wejnert et al., 2010). As within similar settings characterized by seasonal upwelling, *G. bulloides* appears to migrate slightly deeper in the summer (Wejnert et al., 2010). The average calcification depth of 40 m for *G. menardii* is within the thermocline and the chlorophyll maximum in the GoT, consistent with the observations of Fairbanks et al. (1982).

None of the published relationships between Mg/Ca and calcification temperature used here yield temperatures that correspond to predicted calcification depth for any of the species (Supplementary Content, Fig. S1). The raw Mg/Ca ratios for both *G. bulloides* and *G. ruber* in the GoT are somewhat higher than reported in other studies (Anand et al., 2003; Cléroux et al., 2008; Dekens et al., 2002; Elderfield and Ganssen, 2000). Consequently, depending on the calibration used, for *G. ruber*, Mg/Ca temperatures overestimate SST by an average of 0.2°–6.5 °C (maximum of 14 °C), while the regressions for *G. bulloides* display a wide variability of temperature ranges (Supplementary Content, Fig. S1). The fit between Mg/Ca-based temperatures and surface/mixed layer temperatures for all of the existing equations is poor ($r^2 = 0.07$ for *G. ruber* and $r^2 = 0.15$–0.17 for *G. bulloides*).

Only one study has generated a species-specific equation for *G. menardii* (Eq. (22), Regenberg et al., 2009). The other two are from multi-species equations. Equation (22) (Regenberg et al., 2009) and eq. (24) (Anand et al., 2003) result in temperatures that agree well with one another, but not with temperature at 40 m. Equation (23) (Elderfield and Ganssen, 2000), on the other hand, more closely tracks temperature at 40 m. The fit between Mg/Ca-derived temperatures and temperatures at 40 m for all equations is, as with the other two species, poor ($r^2 = 0.008$).

A simple comparison of the δ^{18}O and Mg/Ca data reveals scatter in the relationship between the two, particularly for samples with Mg/Ca >7 mmol/mol (Supplementary Content, Fig. S2). This scatter could be due to a number of factors, including secondary alteration of one or both of the geochemical proxies, and/or a strong secondary influence by an environmental factor on either δ^{18}O or Mg/Ca in the GoT. In the following sections, we explore these scenarios and attempt to resolve the controls on planktonic foraminiferal geochemistry in this region.

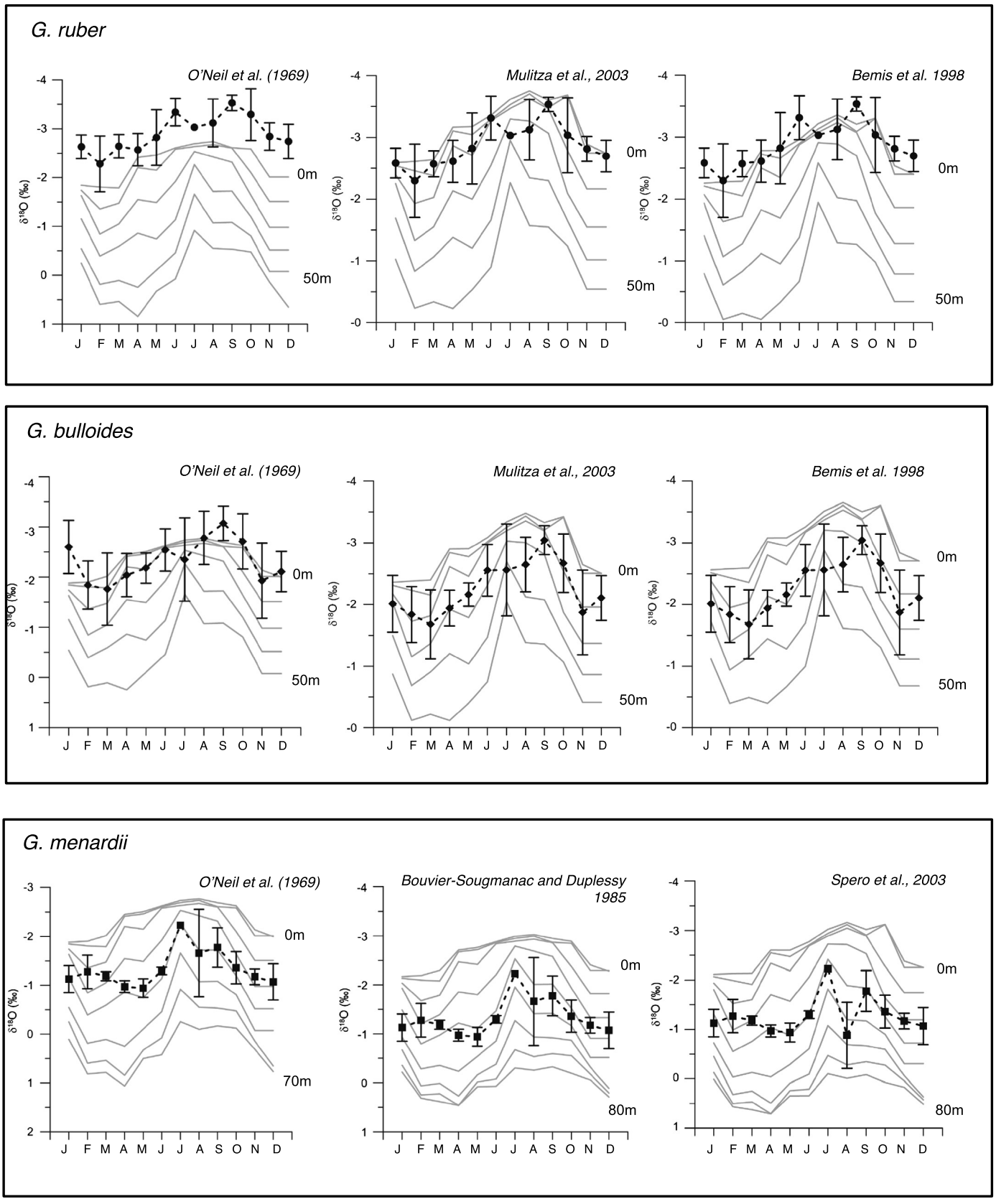

Fig. 3. Average habitat depth for *G. bulloides*, *G. ruber*, and *G. menardii* based on $\delta^{18}O_{calcite}$:temperature relationships found in Table 2. Gray contour lines indicate predicted equilibrium $\delta^{18}O_{calcite}$ at 10 m-intervals based on temperature and calculated $d^{18}O_{sw}$ for each depth interval (depths top and bottom isopleth indicated). Black dashed lines represent average $\delta^{18}O_{calcite}$ per month for each species over the full time series, while error bars indicate the range of $\delta^{18}O_{calcite}$ within each month over the full length of the time series. Sources for each temperature:$\delta^{18}O_{calcite}$ relationship is indicated. Note the change in *y*-axes for the O'Neil et al. (1969) regressions.

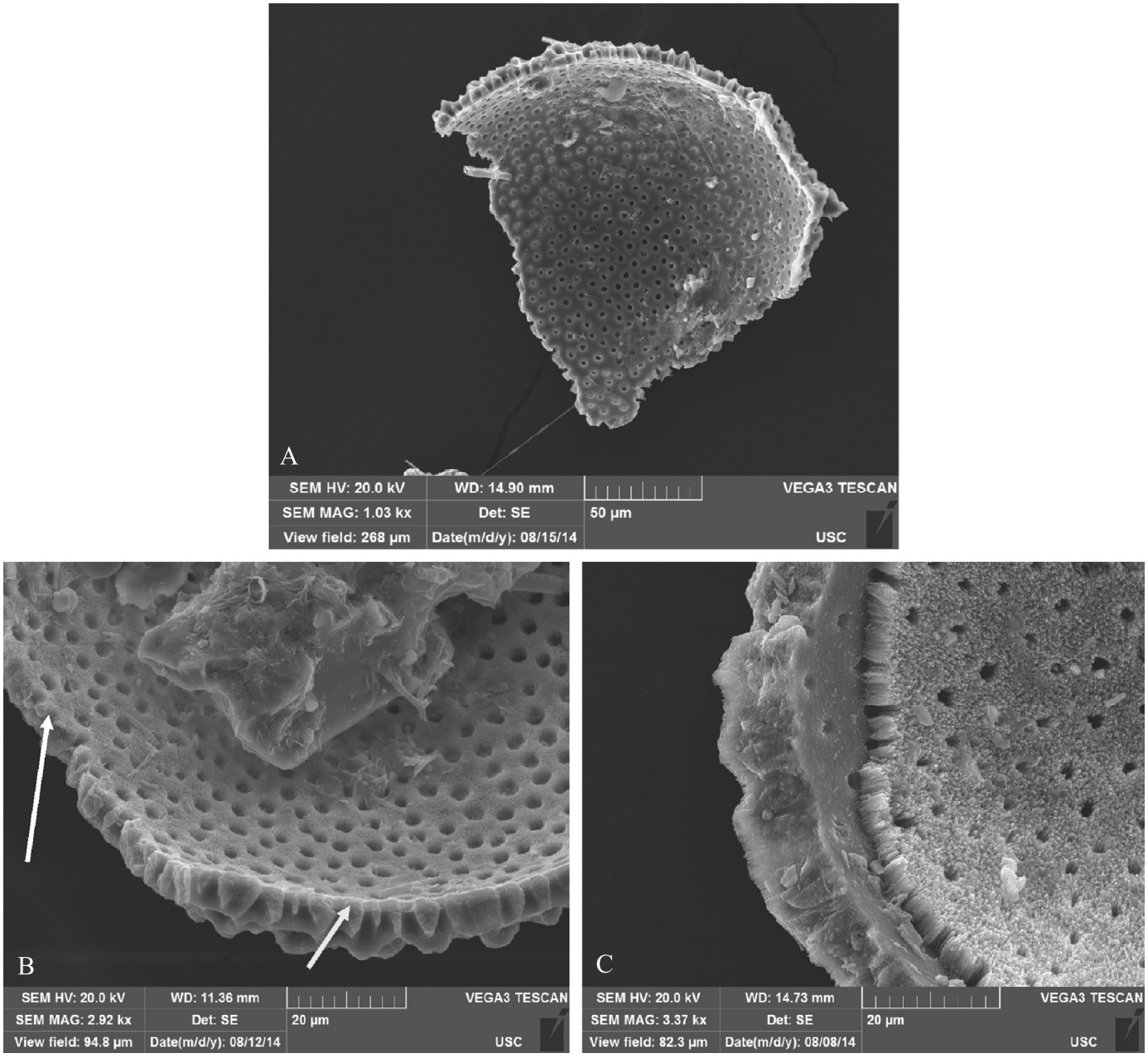

Fig. 4. Test textures of *G. bulloides* with low (<6 mmol/mol), intermediate (6–9 mmol/mol) and high (>9 mmol/mol) Mg/Ca ratios. Specimens with lower Mg/Ca ratios (A) are noticeably thinner and do not have a secondary precipitate. Specimens with very elevated Mg/Ca ratios (C) are characterized by the presence of a secondary calcite precipitate. The individual with an intermediate Mg/Ca ratio has a thin layer of secondary precipitate on the inner surface of its test (B) (indicated by white arrows), with a similar, although finer texture to the precipitate found in (C). Additional SEM results of individuals from samples with low, medium, and high Mg/Ca ratios (not shown) confirm variation in the thickness and spatial extent of the secondary calcification, suggesting a range of alteration that may influence much of the Mg/Ca data we present here. Note the change in scale in image A.

5.2. Influences on foraminiferal $\delta^{18}O$ in the GoT

5.2.1. Seasonal upwelling and $\delta^{18}O_{sw}$ variability

The GoT experiences turbulent mixing and upwelling of subsurface waters. Nevertheless, we use a single relationship to calculate $\delta^{18}O_{sw}$ from salinity (Fairbanks et al., 1982), which does not consider differences in SSS vs $\delta^{18}O_{sw}$ between water sources. For instance, water masses in the upper water column of the GoT are Equatorial Surface Water (ESW) and Subtropical Subsurface Water (SSW) (Machain-Castillo et al., 2008), the latter of which originates in the South Pacific and is characterized by a salinity maximum and different freshwater end member. In the GoT, ESW is typically found in the upper 55–70 m of the water column although during the winter and spring, ESW shoals to 35–50 m (Machain-Castillo et al., 2008).

To evaluate the potential impact of seasonal upwelling of SSW on our depth habitat calculations, we use a $\delta^{18}O_{sw}$:salinity relationship for subsurface waters (40–400 m) from the Panama Bight (1–10°N; 75–90°W) (Benway and Mix, 2004), and compute equilibrium $\delta^{18}O_{calcite}$ for the winter months with a SSW $\delta^{18}O_{sw}$. Benway and Mix (2004) report that this water mass upwells in the eastern equatorial Pacific and Costa Rica Dome, so it may be appropriate for calculating SSW $\delta^{18}O_{sw}$ here.

$$\delta^{18}O_{sw} = 0.424 * S - 16.5 \quad (25)$$

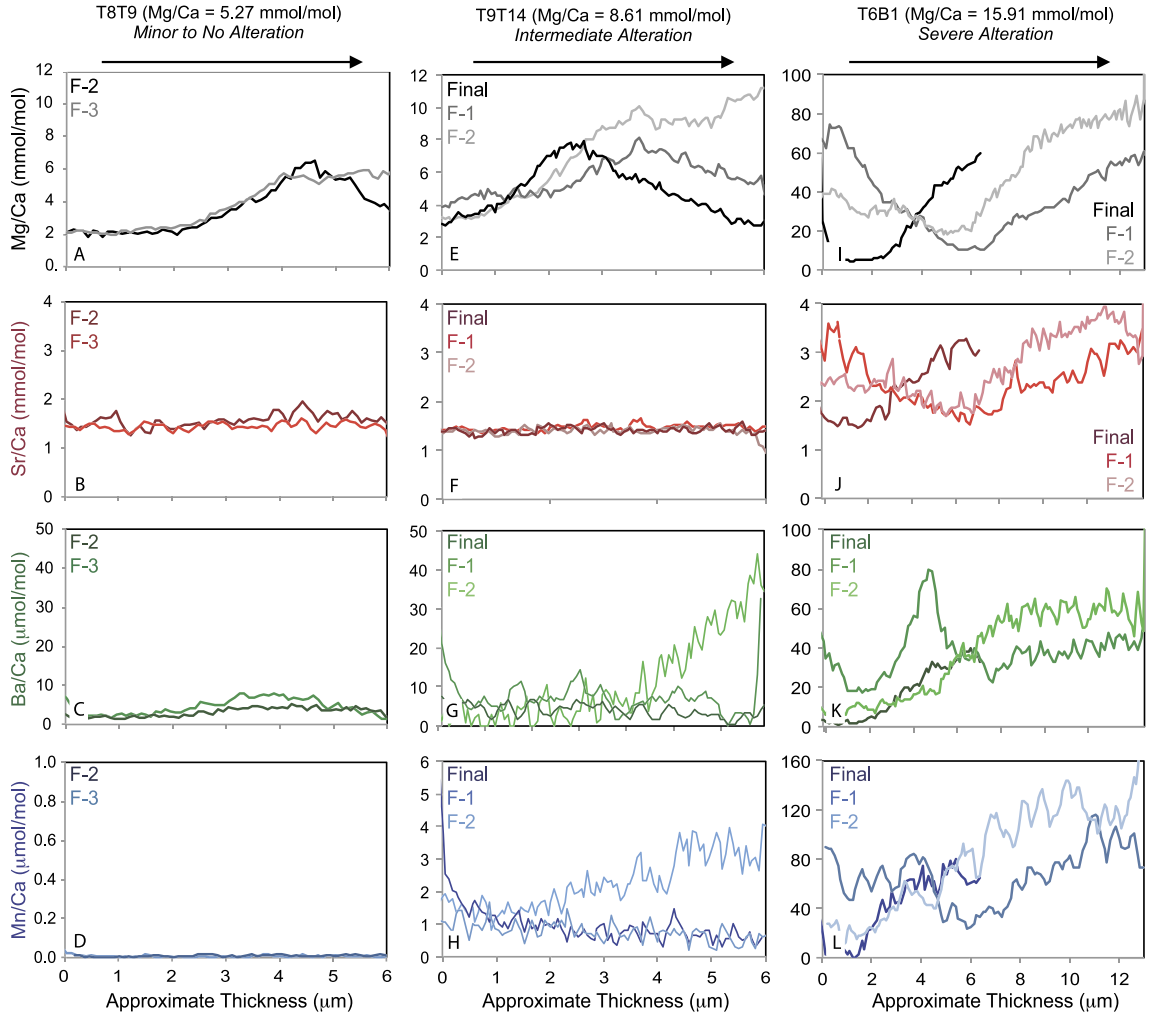

Fig. 5. LA-ICPMS Mg/Ca, Sr/Ca, Ba/Ca, and Mn/Ca results for *G. bulloides* specimens from samples with high, intermediate and low solution Mg/Ca ratios. A, B, C, and D: Chamber profiles (f-2 and f-3) for a sample with low solution Mg/Ca ratios and no evidence of secondary calcite. E, F, G, and H. Chamber profiles (f, f-1, and f-2) for an individual from a sample with an intermediate solution Mg/Ca ratio and evidence of secondary calcite precipitate. The TE/Ca ratios generally increase with chamber depth, and decrease in subsequent chambers. I, J, K, and H. Chamber profiles (f, f-1, and f-2) for an individual from a sample with a high solution Mg/Ca ratio and extensive secondary calcite precipitate. Note the scale for the *y*-axes differs for each plot. The TE/Ca ratios in the altered foraminifera are up to an order of magnitude higher within the secondary calcite compared to the primary calcite. Arrows at the top of each panel indicate direction of laser analysis, from the outside to inside of the shell.

Using Eq. (25) to calculate $\delta^{18}O_{calcite}$ for the upwelling months (December–March) results in very little change to calcification depths for all three species. Between the surface and 50 m, the predicted $\delta^{18}O_{calcite}$ values decrease by 0.1–0.3‰, while below 50 m water depth, the values change by 0.01–0.02‰. These slight changes in $\delta^{18}O$ have no appreciable influence on calcification depth, shifting wintertime habitats by ~5 m.

5.2.2. $pH/[CO_3^{2-}]$

Our calculated mixed layer (0–30 m) $[CO_3^{2-}]$ values range from ~73–118 μmol/kg, with lower values (73–83 μmol/kg) during the winter/spring and higher values (100–118 μmol/kg) during the summer/fall. The corresponding pH values are ~7.6 for the winter/spring, and 7.7–8.0 for the summer/fall. While low compared to ambient seawater pH (8.1), these values agree reasonably well with recently measured pH values in the GoT (Chapa-Balcorta et al., 2015), especially during mixing/upwelling conditions. Between 50–100 m, $[CO_3^{2-}]$ values are more consistent throughout the year and range from ~54–72 μmol/kg (pH of 7.5–7.6). These results are broadly representative of general carbonate chemistry during upwelling and non-upwelling seasons, but are unfortunately not available in a resolution that allows for comparison with the geochemical data over the full time series.

Studies have noted that as $pH/[CO_3^{2-}]$ decreases, $\delta^{18}O$ in several species of planktonic foraminifera also decreases (Spero et al., 1997; Russell and Spero, 2000). Spero et al. (1997) observe, however, that between $[CO_3^{2-}]$ values of 41–100 μmol/kg, there is no change in $\delta^{13}C$ and $\delta^{18}O$ values of their cultured *O. universa*. The mixed layer $[CO_3^{2-}]$ concentrations in the summer/fall (100–118 μmol/kg) in the GoT are at the low end of the range concentrations that are shown to have an influence on $\delta^{18}O$. The lowest $\delta^{18}O$ values in the GoT time series are found in the summer/fall months, suggesting perhaps an influence of low $[CO_3^{2-}]$ on the $\delta^{18}O$ signatures; however, these are the periods of time with warmest SSTs and highest precipitation. It is therefore difficult to decisively determine the influence of pH on $\delta^{18}O$ in these months. The $[CO_3^{2-}]$ values for the remainder of the year, and in subsurface waters, are <100 μmol/kg, the range in which no clear relationship between $[CO_3^{2-}]$ and $\delta^{18}O$ is observed.

5.3. Influences on foraminiferal Mg/Ca in the GoT

5.3.1. Temperature

Because temperatures derived using published Mg/Ca calibrations do not agree with our calculated habitat temperatures, we attempted to generate site-specific Mg/Ca:temperature relationships

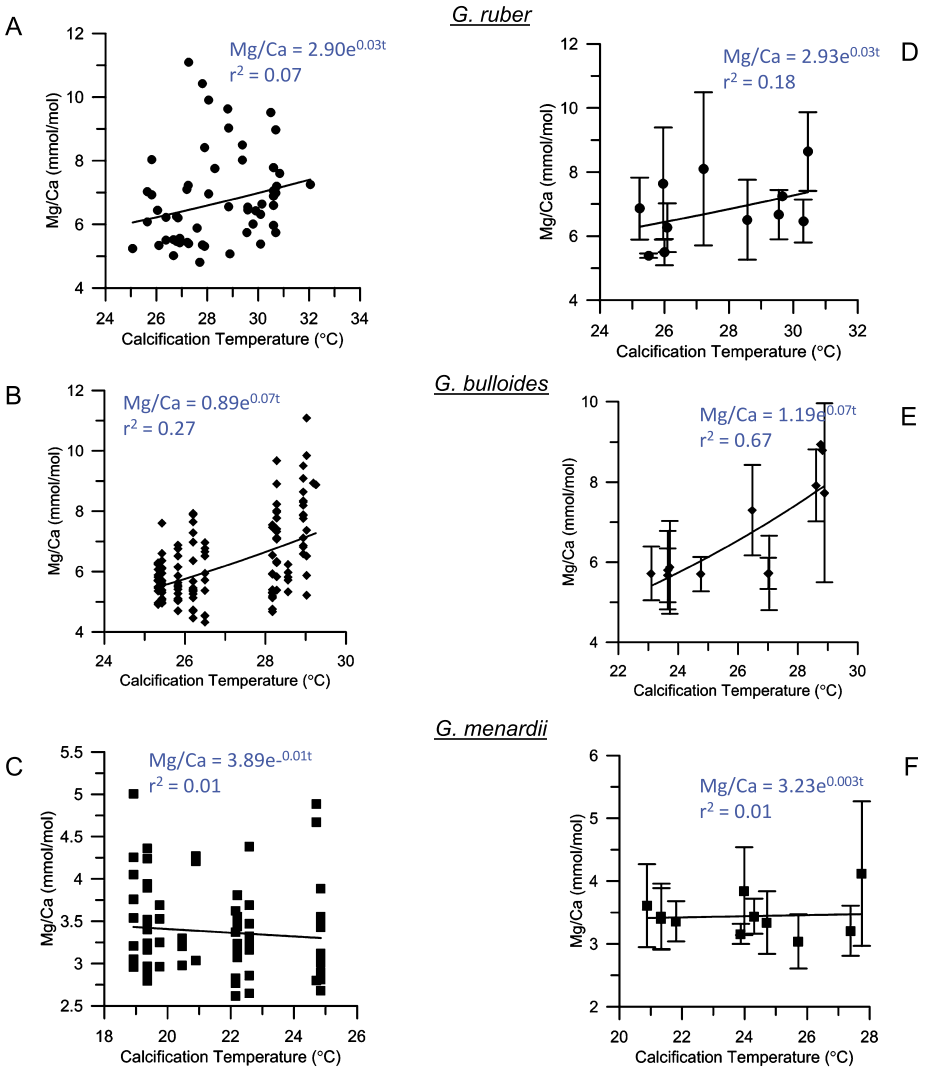

Fig. 6. Relationships between Mg/Ca and average calcification temperature for each species in the Gulf of Tehuantepec. Note the change in scales among plots. Calcification temperature for each species are based on their average calcification depth, calculated in Section 3.4. Because subsurface hydrographic data are only available as one data point per month, the Mg/Ca data for each species were averaged to one data point per month (D–F). The range in Mg/Ca variability for each month is represented by error bars. Relationships between Mg/Ca and temperature for all plots were generated using an exponential fit. (A) All *G. ruber* Mg/Ca and SST (MODIS AQUA). (B) All *G. bulloides* Mg/Ca and temperature at 30 m water depth (WOA 13). (C) All *G. menardii* Mg/Ca and temperature at 40 m water depth (WOA 13). (D) Average Mg/Ca data for *G. ruber* and average SST data per month. (E) Average Mg/Ca data for *G. bulloides* and average temperature data at 30 m per month. (F) Average Mg/Ca data for *G. menardii* and average SST data at 40 m per month. Goodness of fit, preexponential, and exponential constants for each species improve relative to published values with the average values.

(Fig. 6). For each species, we compared Mg/Ca ratios to temperature data at their average δ^{18}O-based calcification depths. While the SST record is at biweekly resolution, our subsurface hydrographic data is only available at monthly resolution. We therefore average all hydrographic data to monthly resolution for ease of comparison, although this predictably smooths out any higher resolution variability. Several CTD casts were taken during sediment trap turnaround cruises; however, the cruises were restricted mostly to the summer months (August 2008, 2011; September 2006, 2009, 2010), with one winter cast (February 2006).

The agreement between WOA 13 and the CTD data is reasonable for the summer months: (±0.3 °C to ±1.3 °C over the upper 40 m). For February, the CTD data are 2–4 °C higher than the WOA 13 data. With only one winter CTD cast during the six-year span of the sediment trap deployment, it is difficult to reconcile this mismatch, but additional subsurface temperature data would undoubtedly improve our calibration efforts. In order to make our geochemical records comparable to the subsurface temperature data, we averaged the Mg/Ca data to a monthly resolution, with the range in Mg/Ca variability in each month represented by error bars (Fig. 6d–f). For comparison, the fits between temperature and unaveraged Mg/Ca data for each species are also plotted in Fig. 6 (a–c). Averaging the Mg/Ca data improves r^2 values for the relationships, but does not strongly influence pre-exponential and exponential constants for each regression (Fig. 6).

Our regressions between Mg/Ca and temperature for all three species are poor. For *G. ruber*, our relationships suggest a temperature dependence of ~3% (Fig. 6a, d), much lower than the canonical 8–10%. The relatively poor fit between SST and *G. ruber* Mg/Ca ($r^2 = 0.07$–0.17) is not improved by plotting the Mg/Ca data with temperatures at depth.

The relationship between Mg/Ca and *G. bulloides* at its average habitat depth of 30 m (Fig. 6b, e) is somewhat better ($r^2 = 0.27$), particularly for the averaged data ($r^2 = 0.67$). Both preexponential (0.89 and 1.19) and exponential (0.07) constants are in better agreement with other studies (Table 2). For the averaged data, the best fit is observed at 40 m water depth ($r^2 = 0.79$). Temperatures in the upper 30 m of the water column exceed 29 °C in the GoT,

Table 2
Equations used to estimate calcification temperature from Mg/Ca for *G. ruber*, *G. bulloides*, and *G. menardii*.

$Mg/Ca = B\exp(AT)$									
Eq. number	Species	Source	Size fraction	B	A	Max Temp. (°C)	Min Temp. (°C)	Avg offset (°C)	Reference
9	*G. ruber*	Sed Trap (NE Pac)	212–355 μm	0.69	0.068	40.9	28.6	5.0	McConnell and Thunell (2005)
10	*G. ruber*	Core Top (SCS)	250–350 μm	0.38	0.089	37.9	32.2	3.8	Hastings et al. (2001)
11	*G. ruber*	Core Top (Trop Pac)	250–350 μm	0.30	0.089	40.6	34.8	6.5	Lea et al. (2000)
12	*G. ruber*	Core Top (N Atl)	250–350 μm	0.38	0.090	37.5	31.8	6.1	Dekens et al. (2002)
13	*G. ruber*	Core Top (Trop Atl)	355–400 μm	0.40	0.940	35.4	29.9	7.4	Regenberg et al. (2009)
14	*G. ruber*	Culture	>500 μm	0.50	0.080	38.8	32.4	4.0	Kısakürek et al. (2008)
15	*G. ruber*	Sed Trap (N Atl)	250–350 μm	0.34	0.102	33.5	28.62	6.3	Anand et al. (2003)
16	*G. bulloides*	Culture	–	0.510	0.104	29.8	20.6	3.0	Lea et al. (1999)
17	*G. bulloides*	Culture + Core Top (Ind/Pac)	250–350 μm	0.470	0.108	29.5	20.7	3.0	Mashiotta et al. (1999)
18	*G. bulloides*	Core Top (N Atl)	250–350 μm	0.780	0.082	32.4	20.1	1.8	Cléroux et al. (2008)
19	*G. bulloides*	Core Top (N Atl)	300–500 μm	0.810	0.081	32.3	20.1	2.0	Elderfield and Ganssen (2000)
20	*G. bulloides*	Sed Trap (NE Pac)	212–355 μm	1.200	0.570	39.0	22.5	1.7	McConnell and Thunell (2005)
21	*G. bulloides*	Sed Trap (NE Pac)	300–450 μm	0.690	0.090	36.4	22.8	0.9	Pak et al. (2004)
22	*G. menardii*	Core Top (Trop Atl)	355–400 μm	0.36	0.910	28.9	21.8	2.9	Regenberg et al. (2009)
23	*G. menardii*	Core Top (N Atl)	–	0.65	0.085	22.7	16.2	2.6	Elderfield and Ganssen (2000)
24	*G. menardii*	Sed Trap (N Atl)	350–500 μm	0.38	0.090	28.7	21.4	2.9	Anand et al. (2003)
SST						32.1	22.1		MODIS AQUA
Temp. at 30 m						29.3	25.3		WOA 13
Temp. at 40 m						27.3	18.9		WOA 13

a range at which scatter in the Mg/Ca:temperature relationship in *G. bulloides* has been observed in previous studies (Elderfield and Ganssen, 2000). McConnell and Thunell (2005), however, found the relationship between Mg/Ca and temperature in G. *bulloides* to remain robust at that temperature range (>29 °C).

Finally, we observe no correlation between *G. menardii* Mg/Ca and temperature at 40 m water depth ($r^2 = 0.01$) (Fig. 6c, f). The fit is not improved when calcification depth is shifted up or down by as much as 30 m. Based on the $\delta^{18}O$ data, *G. menardii* appears to maintain a fairly constant depth throughout the year (40 m), and so would be exposed to an annual temperature range of 9 °C (18.3–27.3 °C).

5.3.2. Salinity

The influence of salinity on foraminiferal Mg/Ca has been an actively debated topic in the field in recent years. Most culture studies have shown that Mg/Ca increases by 4–8% per salinity unit (Hönisch et al., 2013; Kısakürek et al., 2008; Lea et al., 1999). Although results from some field-based studies have suggested a much larger influence (15–57% increase per salinity unit) of salinity on shell Mg/Ca (Arbuszewski et al., 2010; Ferguson et al., 2008), reexamination of study sites, samples, and/or methods has resulted in alternate explanations for elevated Mg/Ca ratios (Hönisch et al., 2013). These include variable calcite preservation within a single ocean basin (Hertzberg and Schmidt, 2013), and changes in seawater carbonate chemistry (van Raden et al., 2011).

To evaluate the potential influence of salinity on Mg/Ca in the GoT, we calculated "excess Mg/Ca" – the difference between measured Mg/Ca and expected Mg/Ca based on calcification temperature. To calculate calcification temperature, we used eq. (4) (Mulitza et al., 2003), eq. (6) (Mulitza et al., 2003), and eq. (8) (Spero et al., 2003) for *G. ruber*, *G. bulloides*, and *G. menardii*, respectively, and Eq. (1) for calculating $\delta^{18}O_{sw}$. To calculate expected Mg/Ca, we used Eq. (24) (Anand et al., 2003) for all three species.

Relationships between excess Mg/Ca and salinity in the GoT are inconsistent (Supplementary Content, Fig. S3). For *G. ruber* and *G. menardii*, we do not observe any relationship between Mg/Ca and salinity although, for *G. bulloides* there is a negative relationship, which is strongest at 20 m water depth ($r^2 = 0.51$). This reflects the fact that the highest excess Mg/Ca for *G. bulloides* occurs during the warmest/wettest months (July–August) in the GoT. If salinity and excess Mg/Ca are positively correlated, our data suggest that, at least during the summer, temperature and not salinity is the overriding control on Mg/Ca. Negative relationships between Mg/Ca and salinity exist for all three species here. Again, this most likely reflects the fact that the highest Mg/Ca ratios occur during the warmest, wettest months, and precludes salinity as an explanation for the misfit between Mg/Ca and temperature in the GoT.

5.3.3. Seawater carbonate chemistry

Some of the *G. bulloides* samples with Mg/Ca ratios >9 mmol/mol are from the transition periods into and out of elevated productivity, as evidenced by pronounced chlorophyll maxima (Fig. 7). These periods occur at the beginning (November) and end (March/April) of the upwelling season and contain samples with exceptionally high $\delta^{18}O_{calcite}$ values. If both proxies were recording temperature, the Mg/Ca ratios during these intervals would suggest temperatures that are 8–11 °C higher than typical winter conditions, while the $\delta^{18}O$ values would suggest precisely the opposite (7–16 °C lower). This contradiction indicates the changes in the shell geochemistry are not driven by temperature. The salinity difference between subsurface and surface waters during March/April and November is minor (<0.5 units) (Fig. 1b) and is not a likely explanation for the elevated $\delta^{18}O$ values. Additionally, there is no clear relationship between salinity and Mg/Ca in the GoT.

Secondary precipitates (Fig. 4) found on the inner shell surfaces of intermediate and high-Mg/Ca specimens of *G. bulloides* have Mg/Ca, Mn/Ca, and Ba/Ca ratios up to an order of magnitude higher than element/Ca ratios in the primary calcite (Fig. 5). Similar layers have been observed in fossil foraminifera, with Mg/Ca and Mn/Ca ratios elevated relative to primary calcite (Pena et al., 2005; Regenberg et al., 2007; van Raden et al., 2011). One explanation for these layers on fossil shells is increased carbonate saturation state in bottom and/or pore waters. In euxinic pore waters of organic-rich sediments, precipitation of inorganic calcite is associated with anaerobic remineralization of organic matter, which increases porewater alkalinity and facilitates the precipitation of $CaCO_3$ (Reimers et al., 1996). In the Caribbean, coatings on foraminifera that had undergone shallow burial were found to have Mg/Ca signatures that were elevated by up to 4–6 times higher than those of the primary calcite (Regenberg et al., 2007), attributed to carbonate dissolution and reprecipitation. In the Panama Basin, Mn-rich inorganic calcite coatings were found on fossil foraminifera that are the result of Mn^{2+}-rich, low oxygen conditions, and remineralization of a high organic carbon flux to the seafloor (Pena et al., 2005).

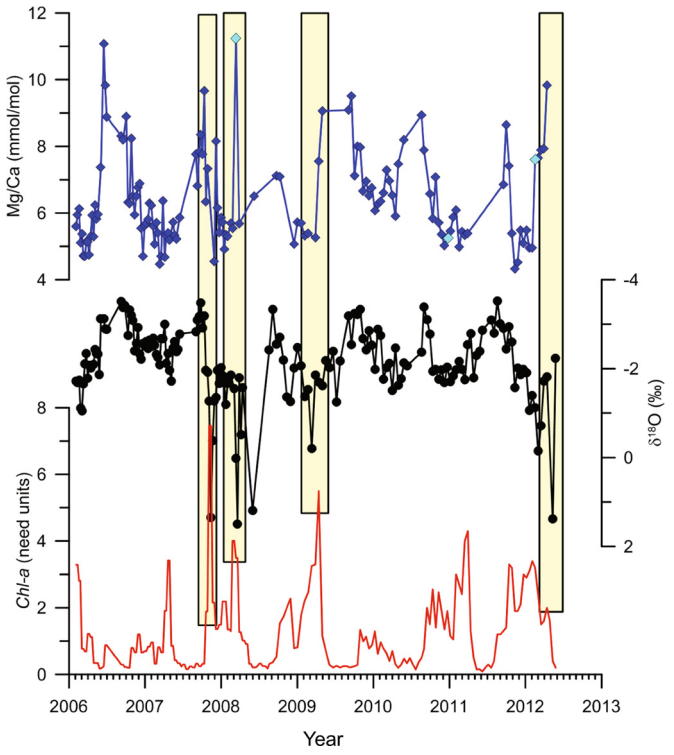

Fig. 7. Mg/Ca, δ^{18}O and Chl-a for *G. bulloides* for the full GoT time series. Periods of peak productivity, indicated by spikes in Chl-a, are often accompanied by samples with elevated Mg/Ca and δ^{18}O values, indicated by yellow boxes. Note that the data presented in these time periods do not always reflect corresponding Mg/Ca-δ^{18}O pairs, due to limitations with sample size, but do suggest that multiple samples from within each period of high productivity have anomalously high values. The representative high, intermediate, and low-Mg/Ca samples from which SEM and LA-ICPMS data are shown are indicated by light blue diamonds on the top panel. (For interpretation of the references to color in this figure legend, the reader is referred to the web version of this article.)

Given the low pH and $[CO_3^{2-}]$ in surface and subsurface waters in the GoT, it at first seems difficult to explain precipitation of inorganic calcite. The GoT is characterized by seasonally high productivity and remineralization of sinking organic matter that leads to suboxic and anoxic conditions in the water column. Although the OMZ is well developed below 200 m in this region, oxygen levels begin to decrease as shallow as 25 m water depth, which is within the range of habitat depths for all three species studied here. During intense mixing events, low oxygen levels may occur at even shallower depths. Importantly, such reduced oxygen levels are unlikely to affect the survival of these planktonic species (Kuroyanagi et al., 2013). Interestingly, these conditions in the water column parallel those found in the sediment column that have been called upon to explain similar alteration in fossil foraminifera (Pena et al., 2005; Regenberg et al., 2007; van Raden et al., 2011). Thus, the high productivity during mixing events may lead to conditions that favor the precipitation of TE/Ca-enriched secondary calcite.

The presence of altered foraminifera in samples from the top and bottom traps that were collected simultaneously indicates that the secondary precipitate we have observed is not an artifact of unusual conditions in a single trap cup, although it is possible that extended storage in the cups prior to recovery may have helped facilitate their precipitation. Measurements of pH in sediment trap cups that were buffered with an identical formalin-sodium borate solution are routinely carried out on samples from the Cariaco Basin, a continental margin site with high rates of primary productivity and an anoxic water column. No changes in pH were observed for collection periods marked by high fluxes of organic carbon flux (Tappa, pers. comm.), suggesting the buffered formalin is generally effective in fixing organic matter and preventing large swings in carbonate chemistry within trap cups.

The LA-ICPMS and SEM results presented here are not an exhaustive representation of altered samples and environmental conditions within this time series. The geochemical signature of the high-Mg/Ca specimen is clearly altered by the secondary calcite, but not every sample with Mg/Ca >9 mmol/mol occurs during a peak in productivity (Fig. 7). Thus, while these periods of high productivity may lead to extremes in water chemistry, it is not clear that they are necessary to facilitate secondary calcite precipitation. Additionally, although it is thinner, the geochemistry of the secondary calcite layer on the specimen with intermediate Mg/Ca (Fig. 4 and 5), likely also influences the bulk TE/Ca ratios of the sample. Given that ~40% of our samples have solution Mg/Ca ratios 6–9 mmol/mol, these results imply that nearly half the time series could be subject to secondary alteration of some degree. Such pervasive alteration could contribute considerably to the misfit between Mg/Ca:calcification temperature in the GoT.

Culture studies have found that decreases in pH and $[CO_3^{2-}]$ influence primary foraminiferal shell element/Ca (Lea et al., 1999; Kısakürek et al., 2008; Russell et al., 2004). For example, Russell et al. (2004) found that below 200 µmol/kg $[CO_3^{2-}]$, Mg/Ca in *G. bulloides* increases as $[CO_3^{2-}]$ decreases, while for *G. ruber*, Kısakürek et al. (2008) observe an ~80% increase in shell Mg/Ca when carbonate ion concentration decreases from 200 to 140 µmol/kg.

Russell et al. (2004) found a 16% increase in *G. bulloides'* Mg/Ca with every 0.1-unit decrease in pH below 8.2. Substituting our calculated pH values (7.6–8.0) into their relationship produces Mg/Ca ratios of ~9 mmol/mol. A recent study by Evans et al. (2016) confirms the trend of increasing Mg/Ca with decreasing pH for multiple species of foraminifera. Using their linear relationship between pH and excess Mg/Ca (Evans et al., 2016) indicates that up to 1.4 mmol/mol of "excess Mg/Ca" in our samples can be explained by the influence of pH. In the GoT, average excess Mg/Ca is 1.09–2.04 for *G. ruber* and 0.61–1.00 for *G. bulloides*.

During periods of high productivity, we have cited increased carbonate saturation state as an explanation for the Mg-enriched secondary precipitate formation. Paradoxically, it seems that low pH and low $[CO_3^{2-}]$ in the surface waters could contribute to the elevated Mg/Ca ratios that occur outside of periods of high primary productivity. Without a more systematic evaluation of the extent and nature of the secondary calcite, it is difficult to separate the relative impact of the two apparently contradictory mechanisms, but it is reasonable to conclude that seawater carbonate chemistry significantly influences planktonic foraminiferal Mg/Ca in the GoT.

5.3.4. Secondary calcification and the δ^{18}O signal

If secondary calcification influences the TE/Ca ratios of the foraminiferal calcite, it stands to reason the primary δ^{18}O signatures could be altered as well, reducing the reliability of using this proxy to reconstruct depth habitats and/or temperatures. Depth (and therefore temperature) and carbonate chemistry of the water column could influence the δ^{18}O of the secondary precipitate. That the precipitate appears to be inorganic should not influence the fractionation of δ^{18}O between the calcite and seawater (O'Neil et al., 1969).

If the secondary calcite were precipitated under elevated $[CO_3^{2-}]$, its δ^{18}O composition could be lower than that of the primary calcite. Based on the relationships determined by Spero et al. (1997), an increase of $[CO_3^{2-}]$ from 100 µmol/kg to 200 µmol/kg would result in a ~0.22‰ decrease in δ^{18}O. This is an ~1 °C change in temperature, and is unlikely to substantially alter our estimates of calcification depth. As previously noted, there was no observed change in foraminiferal δ^{18}O with $[CO_3^{2-}]$ below 100 µmol/kg.

Alternatively, if the alteration is occurring at colder temperatures deeper in the water column, the secondary precipitate could have a higher $\delta^{18}O$ than the primary calcite. There are several samples with unusually high $\delta^{18}O$ (Fig. 7), but if the isotopic enrichment is due to temperature, the secondary calcite would have formed between 5–10 °C, which is lower than WOA 13 temperatures from the upper 100 m of the water column. Given the good agreement between habitat depths calculated here and in other studies, and the minor (~1 °C) influence that carbonate chemistry would have on the secondary $\delta^{18}O$ signature, we believe the $\delta^{18}O$ data are fairly robust, with the exception of select outliers during periods of high primary productivity.

5.4. Regional and broader implications

The difference between the $\delta^{18}O$ values of mixed layer and thermocline-dwellers ($\Delta^{18}O_{sfc\text{-}thermo}$) has been used to examine changes in water column stratification (Niebler et al., 1999). The data for the summer months in the GoT are limited, but the existing data show that $\Delta^{18}O_{sfc\text{-}thermo}$ increases during the summer months (Fig. 2d) when the water column is stratified. The gradient decreases to as low as zero during the winter months (December to February) when the water column is well mixed, suggesting that this proxy can be used to detect changes in water column stratification in this region.

During El Niño years, there is an increase in average monthly wind speed and frequency/strength of Tehuanos events in the GoT (Romero-Centeno et al., 2003), which results in a higher frequency and/or duration of mixing events. One strong El Niño event (2009/10) occurred during our study period. In our record, the lowest $\Delta^{18}O_{sfc\text{-}thermo}$ is observed during peak El Niño conditions (Feb–April 2010; Fig. 2d) in agreement with a well-mixed water column at this time. Interestingly, SSTs are warmer in winter/spring of 2010 than in the other winters (Fig. 2) during our study and productivity is lower (Fig. 7), in apparent contradiction to typical upwelling conditions. During El Niño conditions the relaxation of zonal winds results in a deepening of the thermocline in the eastern Pacific. This deepening means that even if there is shallow wind-driven upwelling in the GoT during El Niño conditions, the warmer, nutrient-poor waters from above the thermocline would not support high levels of primary production.

Over the duration of the full time series, there appears to be a decrease in water column stratification as indicated by a decrease in $\Delta^{18}O_{sfc\text{-}thermo}$ ($r^2 = 0.17$) (Fig. 2d). To confirm this trend is not due to a lack of data from the well-stratified summer months in the latter portion of the record, we plotted the change in $\Delta^{18}O_{sfc\text{-}thermo}$ for each calendar month from 2006–2102 (Supplementary Content, Fig. S4). Over the six-year period, for January–June and September–November, a decrease in $\Delta^{18}O_{sfc\text{-}thermo}$ is observed ($r^2 = 0.18$–0.95). This decrease is particularly evident at the start (Oct–Nov) and end (Feb–Apr) of the winter upwelling season. While no data exist for July, August is marked by an increase in $\Delta^{18}O_{sfc\text{-}thermo}$ ($r^2 = 0.98$, $n = 3$), suggesting an increase in stratification during the middle of the rainy season during the study period.

This decreasing trend in stratification is also supported by commensurate decreases in planktonic foraminiferal shell weight for *G. bulloides*, which has been shown to have a positive relationship with ambient $[CO_3^{2-}]$ (Russell et al., 2004) (Fig. 2d). A recent study has shown that the GoT is a source of CO_2 to the atmosphere, with a larger ocean-to-atmosphere flux of CO_2 during well-mixed conditions (Chapa-Balcorta et al., 2015). The trends in shell weight and $\Delta^{18}O_{sfc\text{-}thermo}$ suggest increased upward mixing of subsurface water, which are higher in DIC and lower in pH than surface waters (Chapa-Balcorta et al., 2015), would increase the role of the GoT as a source of CO_2 to the atmosphere as well as influence seawater carbonate chemistry.

6. Summary

In the Gulf of Tehuantepec, *G. ruber* and *G. bulloides* record mixed layer conditions, and *G. menardii* calcifies within the thermocline. Differences in $\delta^{18}O$ between mixed-layer and thermocline dwelling species suggests that turbulent mixing increases during El Niño conditions in the GoT, although basin-wide deepening of the thermocline results in upward mixing of warm, nutrient-poor waters that do not support high primary production. An overall decrease in water column stratification combined with a decrease in foraminiferal shell weight throughout the study period suggests that surface and subsurface $[CO_3^{2-}]$ are decreasing, and the GoT may increasingly act as a source of CO_2 to the atmosphere if recent trends continue.

In the GoT, we observe poor relationships between planktonic foraminiferal Mg/Ca and calcification temperature. We speculate that carbonate chemistry exerts an influence on foraminiferal TE/Ca in the GoT. First, the low pH and $[CO_3^{2-}]$ concentrations in the surface waters of the GoT may exert an influence on primary calcite Mg/Ca, resulting in a trend of higher Mg/Ca ratios for all three species studied here. Additionally, the presence of an inorganic layer of abiogenically precipitated calcite, enriched in Mg/Ca by up to an order of magnitude relative to the primary foraminiferal calcite, is found on shells, some of which were collected during periods of high productivity. The precipitation of this inorganic calcite is similar to what has been observed on the seafloor or in sediments, associated with waters that are supersaturated with respect to calcium carbonate, often in high-productivity, low-oxygen environments. The presence of this layer in sediment trap samples suggests that the similar precipitate found seafloor samples could form in the water column prior to deposition on the seafloor.

As seawater carbonate chemistry changes in response to warming trends, the influence of changing $[CO_3^{2-}]$ on geochemical proxies in foraminifera may become an increasingly important factor to consider in paleoreconstructions. This study highlights the potential for empty foraminiferal shells to be influenced by changes in the carbonate saturation state of the water column prior to deposition on the seafloor.

Acknowledgements

Ship time on board the ROV “El Puma” was financed by the Universidad Nacional Autónoma de México. The authors thank the scientific party and crew for their help. We also thank Alejandro Rodriguez-Ramirez for lab assistance.

Appendix A. Supplementary material

Supplementary material related to this article can be found online at http://dx.doi.org/10.1016/j.epsl.2016.07.039.

References

Anand, P., Elderfield, H., Conte, M.H., 2003. Calibration of Mg/Ca thermometry in planktonic foraminifera from a sediment trap time series. Paleoceanography 18 (2), 1050. http://dx.doi.org/10.1029/2002PA000846.

Anand, P., Elderfield, H., 2005. Variability of Mg/Ca and Sr/Ca between and within the planktonic foraminifers *Globigerina bulloides* and *Globorotalia truncatulinoides*. Geochem. Geophys. Geosyst. 6 (11), Q11D15. http://dx.doi.org/10.1029/2004GC000811.

Antoine, D., André, J.-M., Morel, A., 1996. Oceanic primary production: 2. Estimation at global scale from satellite (Coastal Zone Color Scanner) chlorophyll. Glob. Biogeochem. Cycles 10 (1), 57–69. http://dx.doi.org/10.1029/95GB02832.

Antonov, J.I., Locarnini, R.A., Boyer, T.P., Mishonov, A.V., Garcia, H.E., 2006. World Ocean Atlas 2005, Volume 2: Salinity. Levitus, S. (Ed.), NOAA Atlas NESDIS, vol. 62. U.S. Government Printing Office, Washington, DC, 182 pp. ftp://ftp.nodc.noaa.gov/pub/WOA05/DOC/woa05_salinity_final.pdf.

Arbuszewski, J., deMenocal, P., Kaplan, A., Farmer, E.C., 2010. On the fidelity of shell-derived δ^{18}O seawater estimates. Earth Planet. Sci. Lett. 300 (3–4), 185–196. http://dx.doi.org/10.1016/j.epsl.2010.10.035.

Barker, S., Greaves, M., Elderfield, H., 2003. A study of cleaning procedures used for foraminiferal Mg/Ca paleothermometry. Geochem. Geophys. Geosyst. 4 (9). http://dx.doi.org/10.1029/2003GC000559.

Bemis, B.E., Spero, H.J., Bijma, J., Lea, D.W., 1998. Reevaluation of the oxygen isotopic composition of planktonic foraminifera; experimental results and revised paleotemperature equations. Paleoceanography 13, 150–160. http://dx.doi.org/10.1029/98PA00070.

Benway, H.M., Mix, A.C., 2004. Oxygen isotopes, upper-ocean salinity, and precipitation sources in the eastern tropical Pacific. Earth Planet. Sci. Lett. 224 (3–4), 493–507. http://dx.doi.org/10.1016/j.epsl.2004.05.014.

Bolton, A., Baker, J.A., Dunbar, G.B., Carter, L., Smith, E.G.C., Neil, H.L., 2011. Environmental versus biological controls on Mg/Ca variability in *Globigerinoides ruber* (white) from core top and plankton tow samples in the southwest Pacific Ocean. Paleoceanography 26 (2), PA2219. http://dx.doi.org/10.1029/2010PA001924.

Bouvier-Soumagnac, Y., Duplessy, J.C., 1985. Carbon and oxygen isotopic composition of planktonic foraminifera from laboratory culture, plankton tows, and recent sediment: implications for the reconstruction of paleoclimatic conditions and of the global carbon cycle. J. Foraminiferal Res. 15, 302–320. http://dx.doi.org/10.2113/gsjfr.15.4.302.

Chapa-Balcorta, C., Hernandez-Ayon, J., Durazo, R., Beier, W., Alin, S.R., Lopez-Perez, A., 2015. Influence of post-Tehuano oceanographic processes in the dynamics of the CO_2 system in the Gulf of Tehuantepec, Mexico. J. Geophys. Res., Oceans. http://dx.doi.org/10.1002/2015JC011249.

Cléroux, C., Cortijo, E., Anand, P., Labeyrie, L., Bassinot, F., Caillon, N., Duplessy, J.-C., 2008. Mg/Ca and Sr/Ca ratios in planktonic foraminifera: proxies for upper water column temperature reconstruction. Paleoceanography 23 (3), PA3214. http://dx.doi.org/10.1029/2007PA001505.

Dekens, P.S., Lea, D.W., Pak, D.K., Spero, H.J., 2002. Core top calibration of Mg/Ca in tropical foraminifera: refining paleotemperature estimation. Geochem. Geophys. Geosyst. 3 (4), 1022. http://dx.doi.org/10.1029/2001GC000200.

Dickson, A.G., Millero, F.J., 1987. A comparison of the equilibrium-constants for the dissociation of carbonic-acid in seawater media. Deep-Sea Res., A, Oceanogr. Res. Pap. 34 (10), 1733–1743. http://dx.doi.org/10.1016/0198-0149(87)90021-5.

Elderfield, H., Ganssen, G., 2000. Past temperature and δ^{18}O of surface ocean waters inferred from foraminiferal Mg/Ca ratios. Nature 405, 442–445. http://dx.doi.org/10.1038/35013033.

Evans, D., Wade, B.S., Henehan, M., Erez, J., Müller, W., 2016. Revisiting carbonate chemistry controls on planktic foraminifera Mg/Ca: implications for sea surface temperature and hydrology shifts over the Paleocene–Eocene Thermal Maximum and Eocene–Oligocene transition. Clim. Past 12 (4), 819–835. http://dx.doi.org/10.5194/cp-12-819-2016.

Fairbanks, R.G., Sverdlove, M., Free, R., Wiebe, P.H., Be, A.W.H., 1982. Vertical distribution and isotopic fractionation of living planktonic foraminifera from the Panama Basin. Nature 298 (5877), 841–844. http://dx.doi.org/10.1038/298841a0.

Fehrenbacher, J.S., Spero, H.J., Russell, A.D., Vetter, L., Eggins, S., 2015. Optimizing LA-ICP-MS analytical procedures for elemental depth profiling of foraminifera shells. Chem. Geol. 407–408, 2–9. http://dx.doi.org/10.1016/j.chemgeo.2015.04.007.

Ferguson, J.E., Henderson, G.M., Kucera, M., Rickaby, R.E.M., 2008. Systematic change of foraminiferal Mg/Ca ratios across a strong salinity gradient. Earth Planet. Sci. Lett. 265, 153–166. http://dx.doi.org/10.1016/j.epsl.2007.10.011.

Garcia-Reyes, M., Sydeman, W.J., Schoeman, D.S., Rykaczewski, R., Black, B.A., Smit, A.J., Bograd, S.J., 2015. Under pressure: climate change, upwelling, and eastern boundary upwelling systems. Front. Mar. Sci. 2 (109). http://dx.doi.org/10.3389/fmars.2015.00109.

Goyet, C., Healy, R.J., Ryan, J.P., 2000. Global distribution of total inorganic carbon and total alkalinity below the deepest winter mixed layer depths. ORNL/CDIAC-127, NDP-076. Carbon Dioxide Information Analysis Center, Oak Ridge National Laboratory, U.S. Department of Energy, Oak Ridge, Tennessee. http://cdiac.esd.ornl.gov/oceans/ndp_076/ndp076.html.

Hastings, D., Kienast, M., Steinke, S., Whitko, A.A., 2001. A comparison of three independent paleotemperature estimates from a high resolution record of deglacial SST records in the tropical South China Sea. Eos Trans. AGU 82 (PP12B-10). http://adsabs.harvard.edu/abs/2001AGUFMPP12B..10H.

Hathorne, E.C., James, R.H., Lampitt, R.S., 2009. Environmental versus planktonic foraminifera *G. inflata* and *G. scitula*. Paleoceanography 24 (4), PA4204. http://dx.doi.org/10.1029/2009PA001742.

Hertzberg, J.E., Schmidt, M.W., 2013. Refining *Globigerinoides ruber* Mg/Ca paleothermometry in the Atlantic Ocean. Earth Planet. Sci. Lett. 383, 123–133. http://dx.doi.org/10.1016/j.epsl.2013.09.044.

Hönisch, B., Allen, K.A., Russell, A.D., Eggins, S.M., Bijma, J., Spero, H.J., Lea, D.W., Yu, J., 2011. Planktic foraminifers as recorders of seawater Ba/Ca. Mar. Micropaleontol. 79 (1), 52–57. http://dx.doi.org/10.1016/j.marmicro.2011.01.003.

Hönisch, B., Allen, K.A., Lea, D.W., Spero, H.J., Eggins, S.M., Arbuszewski, J., deMenocal, P., Rosenthal, Y., Russell, A.D., Elderfield, H., 2013. The influence of salinity on Mg/Ca in planktic foraminifers – evidence from cultures, core-top sediments and complementary δ^{18}O. Geochim. Cosmochim. Acta 121, 196–213. http://dx.doi.org/10.1016/j.gca.2013.07.028.

Huffman, G.J., Bolvin, D.T., Nelkin, E.J., Wolff, D.B., Adler, R.F., Gu, G., Hong, Y., Bowman, K.P., Stocker, E.F., 2007. The TRMM Multisatellite Precipitation Analysis (TMPA): quasi-global, multiyear, combined-sensor precipitation estimates at fine scales. J. Hydrometeorol. 8 (1), 38–55. http://dx.doi.org/10.1175/JHM560.1.

Kısakürek, B., Eisenhauer, A., Böhm, F., Garbe-Schönberg, D., Erez, J., 2008. Controls on shell Mg/Ca and Sr/Ca in cultured planktonic foraminiferan, *Globigerinoides ruber* (white). Earth Planet. Sci. Lett. 273 (3–4), 260–269. http://dx.doi.org/10.1016/j.epsl.2008.06.026.

Kuroyanagi, A., da Rocha, R.E., Bijma, J., Spero, H.J., Russell, A.D., Eggins, S.M., Kawahata, H., 2013. Effect of dissolved oxygen concentration on planktonic foraminifera through laboratory culture experiments and implications for oceanic anoxic events. Mar. Micropaleontol. 101, 28–32. http://dx.doi.org/10.1016/j.marmicro.2013.04.005.

Lea, D.W., Mashiotta, T.A., Spero, H.J., 1999. Controls on magnesium and strontium uptake in planktonic foraminifera determined by live culturing – mineralogy and chemistry. Geochim. Cosmochim. Acta 63, 2369–2379. http://dx.doi.org/10.1016/S0016-7037(99)00197-0.

Lea, D.W., Pak, D.K., Spero, H.J., 2000. Climate impact of late Quaternary Equatorial Pacific sea surface temperature variations. Science 289, 1719–1724. http://dx.doi.org/10.1126/science.289.5485.1719.

LeGrande, A.N., Schmidt, G.A., 2006. Global gridded data set of the oxygen isotopic composition in seawater. Geophys. Res. Lett. 33 (12). http://dx.doi.org/10.1029/2006GL026011.

Liang, J.-H., McWilliams, J.C., Gruber, N., 2009. High-frequency response of the ocean to mountain gap winds in the northeastern tropical Pacific. J. Geophys. Res., Oceans 114 (C12). http://dx.doi.org/10.1029/2009JC005370.

Longerich, H.P., Jackson, S.J., Gunther, D., 1996. Laser ablation inductively coupled plasma mass spectrometric transient signal data acquisition and analyte concentration calculation. J. Anal. At. Spectrom. 11, 899–904. http://dx.doi.org/10.1039/JA9961100899.

Machain-Castillo, M.L., Monreal-Gómez, M.A., Arellano-Torres, E., Merino-Ibarra, M., González-Chávez, G., 2008. Recent planktonic foraminiferal distribution patterns and their relation to hydrographic conditions of the Gulf of Tehuantepec, Mexican Pacific. Mar. Micropaleontol. 66 (2), 103–119. http://dx.doi.org/10.1016/j.marmicro.2007.08.003.

Marr, J.P., Baker, J.A., Carter, L., Allan, A.S.R., Dunbar, G.B., Bostock, H.C., 2011. Ecological and temperature controls on Mg/Ca ratios of *Globigerina bulloides* from the southwest Pacific Ocean. Paleoceanography 26 (2), PA2209. http://dx.doi.org/10.1029/2010PA002059.

Martínez-Botí, M.A., Mortyn, P.G., Schmidt, D.N., Vance, D., Field, D.B., 2011. Mg/Ca in foraminifera from plankton tows: evaluation of proxy controls and comparison with core tops. Earth Planet. Sci. Lett. 307 (1–2), 113–125. http://dx.doi.org/10.1016/j.epsl.2011.04.019.

Mashiotta, T.A., Lea, D.W., Spero, H.J., 1999. Glacial–interglacial changes in Subantarctic sea surface temperature and δ^{18}O-water using foraminiferal Mg. Earth Planet. Sci. Lett. 170 (4), 417–432. http://dx.doi.org/10.1016/S0012-821X(99)00116-8.

McConnell, M.C., Thunell, R.C., 2005. Calibration of the planktonic foraminiferal Mg/Ca paleothermometer; sediment trap results from the Guaymas Basin, Gulf of California. Paleoceanography 20. http://dx.doi.org/10.1029/2004PA001077.

Mehrbach, C., Culberso, C., Hawley, J.E., Pytkowic, R.M., 1973. Measurement of apparent dissociation-constants of carbonic-acid in seawater at atmospheric-pressure. Limnol. Oceanogr. 18 (6), 897–907. http://dx.doi.org/10.4319/lo.1973.18.6.0897.

Molina-Cruz, A., Martinez-López, M., 1994. Oceanography of the Gulf of Tehuantepec, Mexico, indicated by Radiolaria remains. Palaeogeogr. Palaeoclimatol. Palaeoecol. 110 (3), 179–195. http://dx.doi.org/10.1016/0031-0182(94)90083-3.

Müller-Karger, F.E., Fuentes-Yaco, C., 2000. Characteristics of wind-generated rings in the eastern tropical Pacific Ocean. J. Geophys. Res., Oceans 105 (C1), 1271–1284. http://dx.doi.org/10.1029/1999JC900257.

Mulitza, S., Boltovskoy, D., Donner, B., Meggers, H., Paul, A., Wefer, G., 2003. Temperature: δ^{18}O relationships of planktonic foraminifera collected from surface waters. Palaeogeogr. Palaeoclimatol. Palaeoecol. 202 (1–2), 143–152. http://dx.doi.org/10.1016/S0031-0182(03)00633-3.

Niebler, H.-S., Hubberten, H.-W., Gersonde, R., 1999. Oxygen isotope values of planktic foraminifera: a tool for the reconstruction of surface water stratification. In: Fischer, G., Wefer, G. (Eds.), Use of Proxies in Paleoceanography – Examples from the South Atlantic. Springer, Berlin.

OBPG, 2002. MODIS Aqua Level 3 SST Thermal IR Monthly 4 km Daytime. Ver. 1. PO.DAAC, CA, USA. Dataset accessed [2014-06-01].

O'Neil, J.R., Clayton, R.N., Mayeda, T.K., 1969. Oxygen isotope fractionation in divalent metal carbonates. J. Chem. Phys. 51 (12), 5547–5558. http://dx.doi.org/10.1063/1.1671982.

Pak, D.K., Lea, D.W., Kennett, J.P., 2004. Seasonal and interannual variation in Santa Barbara Basin water temperatures observed in sediment trap foraminiferal Mg/Ca. Geochem. Geophys. Geosyst. 5 (12), Q12008. http://dx.doi.org/10.1029/2004GC000760.

Pelletier, G., Lewis, E., Wallace, D., 2005. A Calculator for the CO_2 System in Seawater for Microsoft Excel/VBA. Washington State Department of Ecology, Olympia, WA. Brookhaven National Laboratory, Upton, NY.

Pena, L.D., Calvo, E., Cacho, I., Eggins, S., Pelejero, C., 2005. Identification and removal of Mn–Mg-rich contaminant phases on foraminiferal tests: implications for Mg/Ca past temperature reconstructions. Geochem. Geophys. Geosyst. 6 (9), Q09P02. http://dx.doi.org/10.1029/2005GC000930.

Pennington, J.T., Mahoney, K.L., Kuwahara, V.S., Kolber, D.D., Calienes, R., Chavez, F.P., 2006. Primary production in the eastern tropical Pacific: a review. Prog. Oceanogr. 69 (2–4), 285–317. http://dx.doi.org/10.1016/j.pocean.2006.03.012.

Perez-Cruz, L.L., Machain-Castillo, M.L., 1990. Benthic foraminifera of the oxygen minimum zone, continental shelf of the Gulf of Tehuantepec, Mexico. J. Foraminiferal Res. 20 (4), 312–325. http://dx.doi.org/10.2113/gsjfr.20.4.312.

Regenberg, M., Nürnberg, D., Schönfeld, J., Reichart, G.J., 2007. Early diagenetic overprint in Caribbean sediment cores and its effect on the geochemical composition of planktonic foraminifera. Biogeosciences 4, 957–973. http://dx.doi.org/10.5194/bg-4-957-2007.

Regenberg, M., Steph, S., Nürnberg, D., Tiedemann, R., Garbe-Schönberg, D., 2009. Calibrating Mg/Ca ratios of multiple planktonic foraminiferal species with δ^{18}O-calcification temperatures: paleothermometry for the upper water column. Earth Planet. Sci. Lett. 278 (3–4), 324–336. http://dx.doi.org/10.1016/j.epsl.2008.12.019.

Reimers, C.E., Ruttenberg, K.C., Canfield, D.E., Christiansen, M.B., Martin, J.B., 1996. Porewater pH and authigenic phases formed in the uppermost sediments of the Santa Barbara Basin. Geochim. Cosmochim. Acta 60 (21), 4037–4057. http://dx.doi.org/10.1016/S0016-7037(96)00231-1.

Romero-Centeno, R., Zavala-Hidalgo, J., Gallegos, A., O'Brien, J.J., 2003. Isthmus of Tehuantepec Wind Climatology and ENSO Signal. J. Climate 16 (15), 2628–2639. http://dx.doi.org/10.1175/1520-0442(2003)016<2628:IOTWCA>2.0.CO;2.

Russell, A.D., Hönisch, B., Spero, H.J., Lea, D.W., 2004. Effects of seawater carbonate ion concentration and temperature on shell U, Mg, and Sr in cultured planktonic foraminifera. Geochim. Cosmochim. Acta 68 (21), 4347–4361. http://dx.doi.org/10.1016/j.gca.2004.03.013.

Russell, A.D., Spero, H.J., 2000. Field examination of the oceanic carbonate ion effect on stable isotopes in planktonic foraminifera. Paleoceanography 15 (1), 43–52. http://dx.doi.org/10.1029/1998PA000312.

Spero, H.J., Mielke, K.M., Kalve, E.M., Lea, D.W., Pak, D.K., 2003. Multispecies approach to reconstructing eastern Equatorial Pacific thermocline hydrography during the past 360 kyr. Paleoceanography 18, 1022. http://dx.doi.org/10.1029/2002PA000814.

Spero, H.J., Bijma, J., Lea, D.W., Bemis, B.E., 1997. Effect of seawater carbonate concentration on foraminiferal carbon and oxygen isotopes. Nature 390, 497–500. http://dx.doi.org/10.1038/37333.

Steinke, S., Chiu, H.-Y., Yu, P.-S., Shen, C.-C., Löwemark, L., Mii, H.-S., Chen, M.-T., 2005. Mg/Ca ratios of two *Globigerinoides ruber* (white) morphotypes: implications for reconstructing past tropical/subtropical surface water conditions. Geochem. Geophys. Geosyst. 6 (11), Q11005. http://dx.doi.org/10.1029/2005GC000926.

Stumpf, H.G., 1975. Satellite detection of upwelling in the Gulf of Tehuantepec, Mexico. J. Phys. Oceanogr. 5 (2), 383–388. http://dx.doi.org/10.1175/1520-0485(1975)005<0383:SDOUIT>2.0.CO;2.

Thirumalai, K., Richey, J.N., Quinn, T.M., Poore, R.Z., 2014. *Globigerinoides ruber* morphotypes in the Gulf of Mexico: a test of null hypothesis. Sci. Rep. 4, 6018. http://dx.doi.org/10.1038/srep06018.

van Raden, U.J., Groeneveld, J., Raitzsch, M., Kucera, M., 2011. Mg/Ca in the planktonic foraminifera *Globorotalia inflata* and *Globigerinoides bulloides* from Western Mediterranean plankton tow and core top samples. Mar. Micropaleontol. 78 (3–4), 101–112. http://dx.doi.org/10.1016/j.marmicro.2010.11.002.

Wang, L., 2000. Isotopic signals in two morphotypes of *Globigerinoides ruber* (white) from the South China Sea: implications for monsoon climate change during the last glacial cycle. Palaeogeogr. Palaeoclimatol. Palaeoecol. 161 (3–4), 381–394. http://dx.doi.org/10.1016/S0031-0182(00)00094-8.

Wejnert, K.E., Pride, C.J., Thunell, R.C., 2010. The oxygen isotope composition of planktonic foraminifera from the Guaymas Basin, Gulf of California: seasonal, annual, and interspecies variability. Mar. Micropaleontol. 74 (1–2), 29–37. http://dx.doi.org/10.1016/j.marmicro.2009.11.002.

Zweng, M.M., Reagan, J.R., Antonov, J.I., Locarnini, R.A., Mishonov, A.V., Boyer, T.P., Garcia, H.E., Baranova, O.K., Johnson, D.R., Seidov, D., Biddle, M.M., 2013. World Ocean Atlas 2013, Volume 2: Salinity. Levitus, S. (Ed.), Mishonov, A. (Technical Ed.), NOAA Atlas NESDIS, vol. 74. 39 pp. http://data.nodc.noaa.gov/woa/WOA13/DOC/woa13_vol2.pdf.